Available online at www.sciencedirect.com
SCIENCE DIRECT®
Thermochimica Acta 425 (2005) 131–136
thermochimica acta
www.elsevier.com/locate/tca

Reaction kinetics and formation mechanism of magnesium ferrites

Jong-Gyu Paik[a,*], Man-Jong Lee[a], Sang-Hoon Hyun[b]

[a] *Agency for Defense Development, Yousung, P.O. Box 35, Daejon 305-600, Korea*
[b] *Department of Ceramic Engineering, Yonsei University, Sinchon-dong, Seodaemun-gu, Seou, Korea*

Received 26 January 2004; received in revised form 31 May 2004; accepted 24 June 2004
Available online 23 August 2004

Abstract

The reaction kinetics on the spinel formation reaction of Mg–ferrite formation during the heat-treatment of ferric and magnesium oxide powders has been evaluated by both Jander and Ginstling–Brounstein models. It revealed that the spinel formation could be successfully described by Jander's equation. The rate constant calculated by the Jander equation was $3 \times 10^{-6}\,s^{-1}$ at 800 °C and increased to $1.4 \times 10^{-3}\,s^{-1}$ as the reaction temperature increased up to 1000 °C. The activation energy of spinel formation was evaluated to be 335 kJ/mol, which was also confirmed by the differential thermal analysis. The activation energy coincided with that of Mg^{2+} diffusion reaction within MgO lattice suggesting this acted as a rate-determining step in the entire reaction.

Keywords: Hysteresis loop; X-ray diffraction; Activation energy

1. Introduction

Magnesium ferrites ($MgFe_2O_4$), having a spinel structure, show a rectangular hysteresis loop, making them highly suitable for use in the area of memory and switching circuits of digital computers, and in low-loss microwave devices in microwave radar system [1]. Routinely, these ferrites are synthesized by the chemical reaction between mixed oxides, hydroxides or carbonates at a temperature range between 600–1100 °C [2,3], where the reaction products are formed by the thermal diffusion of cations through the ferrite film formed between starting oxides. Because the characteristics of synthesized powders greatly affect the final electromagnetic properties as well as the densification behavior of the sintered ferrites [4–6], kinetic studies of ferrite formation have been reported for the optimization for the ferrite formation reaction [7–11].

The formation mechanism of spinel, which is closely related to diffusion of metal ions, was first studied using $MgAl_2O_4$ reaction by Koch and Wagner [7]. Following Wagner model, the formation of ferrite spinel was explained as a result of the counter diffusion of cations within a rigid oxide lattice formed at the interface of constituent oxides. Carter [8], who used pores as inert markers, stated a supporting idea that $MgFe_2O_4$ is formed by the counter diffusion of Mg^{2+} and Fe^{3+} through a relatively rigid oxide lattice. Meanwhile, Blackman [9] suggested that the diffusing ions might not be Fe^{3+} but Fe^{2+}, based on the observation of Fe^{2+} at the reaction interface. Thus, it is believed that the Fe^{2+} ions can diffuse after the decomposition of Fe_2O_3 into 2FeO and oxygen gas. Also the oxygen moves through the reacted area by vapor transport and then is finally reduced. Reijnen [10] also reported the existence of Fe^{2+} in the reaction surface of MgO + Fe_2O_3 and suggested that oxygen might take part in the reaction as a vapor phase. This idea was supported by Paulus [11] by presenting evidence of Fe^{2+} diffusion.

Meanwhile, the reaction rate is increased by increasing the iron percentage in the initial mixture at all calcination temperatures [8]. This trend is expected because the concentration of vacancies increases with increasing the iron content

* Corresponding author. Tel.: +82 42821 2467; fax: +82 42823 3400.
E-mail address: paikjg@add.re.kr (J.-G. Paik).

0040-6031/$ – see front matter © 2004 Elsevier B.V. All rights reserved.
doi:10.1016/j.tca.2004.06.012

in the samples where three Mg^{2+} ions would be replaced by two Fe^{3+} ions and a vacancy. From this idea, several reports [12–19] have been presented to discuss the role of various dopants on spinel formation. The final conclusion for the enhancement of ferrite spinel formation due to doping with foreign oxides has been attributed to an effective increase in the mobility of reacting cations taking part in the ferrite formation.

The rate of spinel formation reaction is affected by the activation energy of rate determining reaction because it is driven by the diffusion of cations. The determination of the rate determining species, however, has not been reported so far to the best of the authors' knowledge, although it can provide a better understanding as well as control over the formation reaction of spinel. In the present study, we tried to determine the rate determining species in the ferrite spinel formation reaction by analyzing the kinetics of magnesium ferrite formation. More specifically, the kinetics of ferrite spinel formation reaction in the mixed oxide system of MgO and Fe_2O_3 is analyzed using the quantitative X-ray diffraction (XRD) technique. Furthermore, the reaction rate constant and the activation energy of the spinel formation are calculated from the well-known models of the solid-state reaction such as Jander and Ginstling–Brounstein models. Also, the calculated values of the reaction rate constant and the activation energy of the spinel formation are compared with those measured from differential thermal analysis (DTA). Considering the measured and calculated activation energies, the diffusion of Mg^{2+} within MgO is suggested as the rate-determining step in the ferrite formation reaction.

2. Experimental

2.1. Materials

Equimolar proportions of high purity (>99%) Fe_2O_3 and MgO (both from Aldrich Chem. Co.) were well mixed to ensure the homogeneity of the powdered starting materials. A stoichiometric mixture of both oxides having an average particle size of 0.5 μm were mixed for 12 h in an alcoholic medium with zirconia balls, and then dried at 100 °C for 24 h. The homogenized powders were pressed into pellets having less than 2 mm in thickness at a constant pressure ranging from 0.25×10^3 to 4.0×10^3 kg/cm^2. The obtained pellets were rapidly heated (>800 °C/min) in air to a temperature range between 800 and 1000 °C. After the heat-treatment, the samples were quenched to room temperature. The rapid heating and quenching were used in this study to minimize spinel formation during heating and cooling.

2.2. Characterizations

An XRD analysis of heat-treated samples was carried out with a JDX 8030, JEOL Co. X-ray diffractometer. The XRD patterns were obtained with Cu K_α radiation at 40 kV and 30 mA with scanning speed in 2θ of 2.4 min^{-1}.

The fraction (α) of spinel ferrite was evaluated by the internal standard technique [20]. In this technique, the amount of ferrite spinel formation was evaluated by comparing the intensity area ratio (R_x) of samples with those of standard samples. Standard samples were high purity Fe_2O_3 and synthesized $MgFe_2O_4$ that contained 100% spinel phase following the heat treatment at 1200 °C for 4 h. Here, R_x is calculated by the following equation:

$$R_x = \frac{MgFe_2O_4\,(2\,2\,0)}{MgFe_2O_4\,(2\,2\,0) + Fe_2O_3\,(1\,0\,4)} \quad (1)$$

where $MgFe_2O_4$ (2 2 0) is XRD peak intensity area of (2 2 0) plane of $MgFe_2O_4$ and Fe_2O_3 (1 0 4) is XRD peak intensity area of (1 0 4) plane of Fe_2O_3. Because the (3 1 1) peak, the maximum peak of $MgFe_2O_4$ phase, has a similar d value with the (1 1 0) of Fe_2O_3 phase, the (2 2 0) of $MgFe_2O_4$ phase and the (1 0 4) of Fe_2O_3 phase were used in the evaluation of R_x. From the relation between the volume fraction and the R_x of standard samples, the standard curve was obtained (as shown in Fig. 1). Using the curve fitting of data in the standard curve, the volume fraction (α) of spinel formation in the samples is accurately described as a function of the intensity area ratio (R_x) by the following equation with a correlation factor of 0.99622:

$$\alpha = -1.564R_x^4 + 3.210R_x^3 - 1.304R_x^2 + 0.647R_x - 0.004 \quad (2)$$

In this case, the variation of α with R_x was not linear due to the different absorption coefficients of $MgFe_2O_4$ and Fe_2O_3 phases.

DTA of the various specimens was carried out in air atmosphere using Dupont thermal analysis apparatus (Thermal Analist 2100). The rate of heating was in the range of 10–30 °C min^{-1} and a constant amount of sample (40 mg) was analyzed in each run.

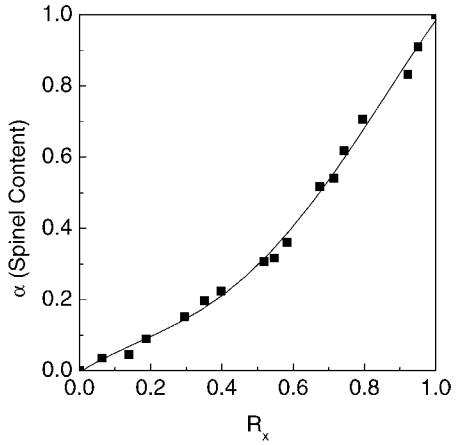

Fig. 1. A standard curve for the determination of the spinel content (volume fraction) obtained from the intensity area ratios (R_x).

3. Results and discussion

3.1. Effect of forming pressure on the ferrite spinel formation

In the analysis of solid-state reaction such as spinel ferrite formation, where the diffusion governs the overall reaction, the contact area of starting materials should be considered as a determining factor. This is because the reacting oxide particles contact each another making at least one of them to diffuse through an increasing product layer at a reaction temperature. Thus, the compaction pressure of powders should be considered because the increase of contact area between powders facilitates the diffusion.

Fig. 2 shows such an effect of powder compaction pressures on the spinel content in Mg ferrites after the heat treatment for 2 h at 900 °C. As can be seen in Fig. 2, the fraction of ferrite spinel after the heat treatment is increased with an increase of forming pressure and reaches to a maximum value of 0.27 regardless of the increase of compaction pressures. Because the fraction of ferrite spinel is constant above a pressure of 2×10^3 kg/cm^2, the forming pressure of samples is set to 2×10^3 kg/cm^2 hereafter.

3.2. Kinetics of ferrite spinel formation

To analyze the kinetics of ferrite spinel formation, the mixed powders compacted at a pressure of 2×10^3 kg/cm^2 were heat-treated at various reaction temperatures for up to 720 min. Fig. 3 shows the XRD analyses of samples heated up to the normal sintering temperature (1300 °C) for 30 min. XRD investigation revealed that spinel phase started to form at 700 °C and its fraction was increased with an increase of heat treatment temperature. After the heat treatment at 1300 °C for 30 min, almost all powders transformed to spinel phase. The Fe_2O_3 phase, however, was still detected even at the normal sintering temperature. Such small amount of remnant Fe_2O_3 plays an important role in the densification

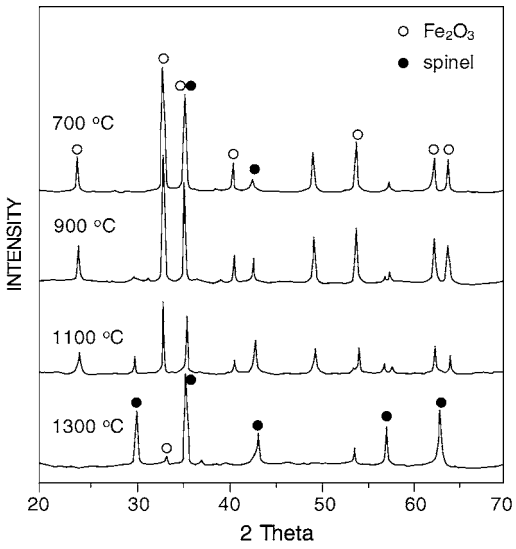

Fig. 3. XRD patterns showing the spinel formed at various reaction temperatures.

of sintered bodies. Ferric ions (Fe^{3+}) in Fe_2O_3 are reduced to ferrous ions (Fe^{2+}) during the sintering process by forming magnetite (Fe_3O_4) or magnesiowustite (MgO·FeO). Because the Fe^{2+} ions diffuse very fast, the final sintered ferrite becomes a microstructure having lots of pores resulting from high driving force for sintering and fast grain growth. Therefore, the control of spinel fraction before the sintering process is important in the final microstructure.

In Fig. 4, the variations of the spinel contents synthesized at various temperature and time are shown. Here, the fraction of ferrite spinel formed was calculated using the intensity area ratio of peaks and the standard curve (see Eq. (2)). Generally, the amount of reaction product at the same reaction temperature tends to increase with the increase of the reaction time. The increasing rate, however, tends to decrease illustrating that the overall reaction of the ferrite spinel is governed by the thermal diffusion of species.

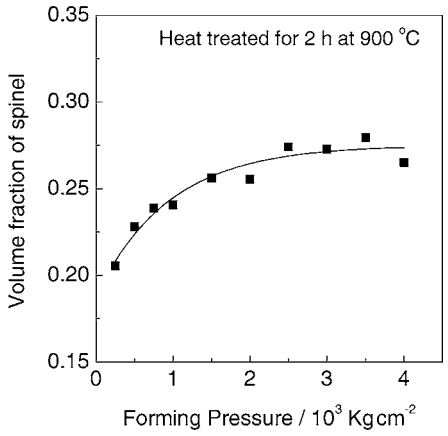

Fig. 2. Variation of the spinel content with increase of compaction pressure after the heat treatment for 2 h at 900 °C.

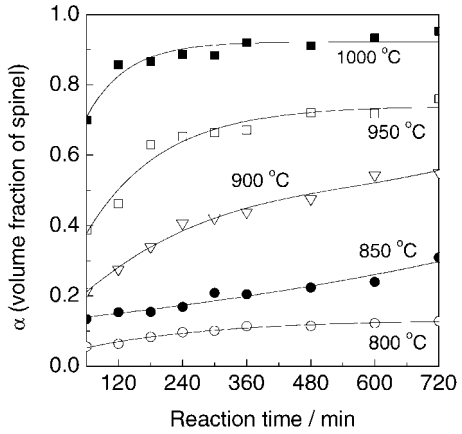

Fig. 4. Variation of spinel content at various reaction temperatures.

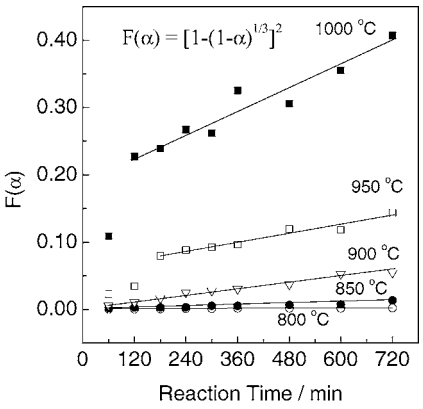

Fig. 5. Data fitted by Jander model at various reaction temperatures.

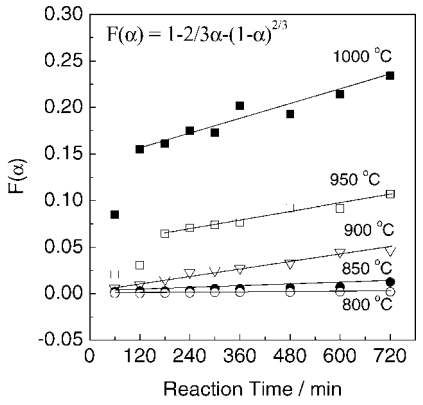

Fig. 6. Data fitted by Ginstling–Brounstein model at various reaction temperatures.

For the detailed kinetics study of the spinel ferrite formation, both Jander [21] and Ginstling–Brounstein [22] equations were applied. In solid-state reactions where diffusion is a rate-determining step, these two models are frequently used in the analysis of reaction mechanism. Jander model analyzes the condition of plane diffusion, Ginstling–Brounstein model uses spherical diffusion.

Fig. 5 shows the ferrite fraction, $F(\alpha)$ calculated from Jander equation:

$$[1-(1-\alpha_A)^{1/3}]^2 = kt \quad (3)$$

where, α_A denotes the fractional volume reacted, k the reaction rate constant, and t time. Up to 900 °C, synthesized ferrite fraction was well explained by the model equation. Above this temperature, however, it deviated from the model equation probably due to large amount of spinel fraction formed at this high temperature. Fig. 6 shows the variation of ferrite fraction, $F(\alpha)$ calculated from Ginstling–Brounstein equation:

$$1-\tfrac{2}{3}\alpha_A-(1-\alpha_A)^{1/3} = kt \quad (4)$$

In this case, a similar result has been observed. Notice the boundary conditions of both models are limited only in the initial stage where the reacted layer is thin. As the ferrite fraction increases, the plane diffusion condition in Jander model and the sphere diffusion condition in Ginstling–Brounstein model are far from their boundary conditions. Thus, at high temperature, those two models could not describe the reaction satisfactorily.

By the least square method, the reaction rate constant (k) of the spinel ferrite formation was calculated. The reaction rate constant and the standard deviations between calculated and measured synthesized fraction are shown in Table 1. The reaction rate constants were similar to each other up to 900 °C. However, these values show considerable differences at 1000 °C. Considering the standard deviations, the Jander model fits better than the Ginstling–Brounstein model.

3.3. Activation energy

Calculations of the activation energy (Q_E) on the basis of Arrhenius equation ($\ln k = -Q_E/RT + \ln C$) were performed, as shown in Fig. 7. Fig. 7 also shows a good agreement up to 900 °C. Above this temperature, both models deviate from linearity. In case of the Ginstling–Brounstein model, the deviation is more severe. The activation energies calculated from the Jander model and the Ginstling–Brounstein model were 335 kJ/mol and 276 kJ/mol, respectively.

To verify the accuracy of the activation energy obtained from the solid state reaction kinetics models, the activation energy was experimentally obtained from DTA reported by Ozawa [23] and was compared with those calculated from the models. In Ozawa method, the activation energy (E_a) of the ferrite formation can be obtained by the Arrhenius plot of the relation between the heating rates and the reaction temperatures.

Table 1
Rate constants at various temperatures calculated by two models

Reaction temperature (°C)	Ginstling–Brounstein model		Jander model	
	k (s^{-1})	S.D.[a]	k (s^{-1})	S.D.
800	3.42×10^{-6}	9.57×10^{-3}	3.54×10^{-6}	9.24×10^{-3}
850	1.52×10^{-5}	1.88×10^{-2}	1.63×10^{-5}	1.84×10^{-2}
900	7.38×10^{-5}	1.87×10^{-2}	8.65×10^{-5}	1.31×10^{-2}
950	1.92×10^{-4}	6.68×10^{-2}	2.85×10^{-4}	4.58×10^{-2}
1000	3.99×10^{-4}	1.32×10^{-1}	1.41×10^{-3}	5.48×10^{-2}

[a] S.D.: standard deviation between experimental and calculated spinel contents.

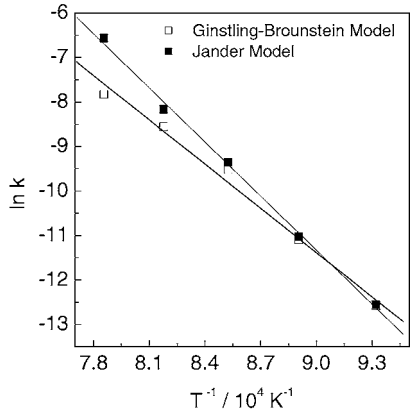

Fig. 7. Plots of the reaction rate constants vs. reciprocal temperature for two models.

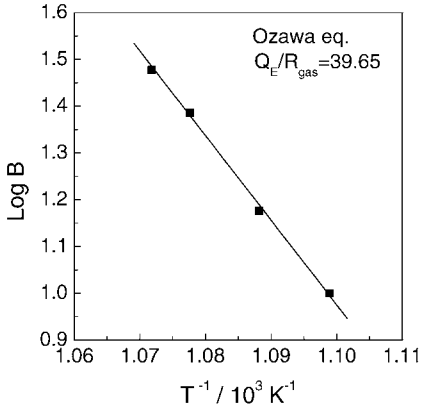

Fig. 9. Plot of the heating rate (B) vs. reciprocal temperature for the calculation of activation energy.

Fig. 8 shows results of DTA for the ferrite spinel formation under the various heating rate of 10, 15, 25 and 30 °C/min. Inspection of the DTA curves with the different heating rates revealed that weak endothermic peaks were detected in all cases at the temperature range of 500–750 °C. As the heating rate increases, the endothermic peaks of the spinel reaction moved toward higher temperature.

The activation energy (E_a) of ferrite formation can be determined by the slope of plots of log of heating rate versus $1/T$ using the following equation:

$$\log B = -0.4567 Q_E/RT + \text{const} \quad (5)$$

where B is the heating rate for differential thermal analysis, R is the gas constant, and T is synthesis temperature. In endothermic reaction, T refers to the minimum position of endothermic peak, i.e. the temperature of 50% reacted. A plot of $\log B$ versus $1/T$ is expected to be linear. Using the slope (see Eq. (5)), the determined activation energy of the reaction was calculated to be 331 kJ/mol by the plot shown in Fig. 9. Comparing the activation energy obtained by DTA with those calculated from the Jander and the Ginstling–Brounstein equations, it can be seen that it coincides with the activation energy (335 kJ/mol) calculated from Jander equation. This denotes that Jander model successfully describes the diffusion relation in present $MgO + Fe_2O_3$ system.

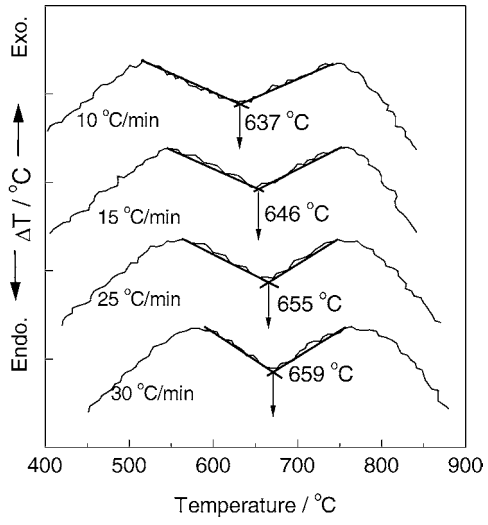

Fig. 8. DTA peaks for the spinel formation reaction at various heating rates.

Spinel ferrite is formed by the diffusion of metal ions (Mg^{2+}, Fe^{2+} and Fe^{3+}) taking part in the reaction. Because Fe^{3+} ions do not diffuse, the whole reaction is governed by the counter diffusion of both Mg^{2+} and Fe^{2+} ions. Meanwhile, the activation energy of whole reaction is determined by the slowest reaction among all the diffusion reactions occurred during the spinel formation. Thus, if one compares the activation energies for the diffusion of such metal ions within their oxides, the rate-determining step can be evaluated. The activation energies for diffusion of Mg^{2+}, Fe^{2+} and Fe^{3+} in their oxides are 327 kJ/mol [24], 126 kJ/mol [25], and 419 kJ/mol [26], respectively. The activation energy obtained in this study coincides with that of Mg^{2+} diffusion in the rigid MgO lattice. Considering the structure of both Mg ferrite and MgO, the diffusion of Mg^{2+} ions within Mg ferrite is much easier compared with that within MgO whose octahedral sites are all filled. This is due to the large number of interstitial vacancies in Mg ferrites structure. Also, considering there is no diffusion related with O^{2-} ions combined with Fe_2O_3 or Fe^{3+} ions, $MgFe_2O_4$ is formed by the counter diffusion of Mg^{2+} and Fe^{2+} through a relatively rigid oxygen lattice, where Mg^{2+} diffusion in the rigid MgO lattice is the rate determining reaction. Dopants that can produce Mg vacancies such as Al_2O_3, Li_2O [18], etc. are expected to enhance the rate of spinel formation because the formed Mg vacancies facilitate Mg^{2+} diffusion within the MgO lattice.

4. Conclusions

Applying Jander and Ginstling–Brounstein equations, the kinetics study of magnesium ferrites are performed. In case of Jander model, the reaction rate constant of the $MgO + Fe_2O_3$ mixture homogeneously compacted under the pressure of 2

$\times 10^3$ kg/cm^2 was 3.5×10^{-6} s^{-1} at 800 °C. This value increased with the increase of the reaction temperature and was 1.4×10^{-3} s^{-1} at 1000 °C. The activation energy of the reaction was also evaluated to be 335 kJ/mol, which is similar to that of Mg^{2+} diffusion in MgO. Comparing the activation energies of self diffusion of Mg^{2+}, Fe^{2+} and Fe^{3+}, the spinel ferrites are formed by the counter diffusion of Mg^{2+} and Fe^{3+} through a relatively rigid oxide lattice. In this case the rate of the whole diffusion reaction is governed by the Mg^{2+} diffusion in the rigid MgO lattice.

References

[1] C. Heck, Magnetic Materials and their Applications, Butterworth, London, 1974.
[2] M. Zenger, Int. J. Mater. Prod. Technol. 9 (1994) 265.
[3] R.E. Kirk, D. Othmer, Encyclopaedia of Chemical Technology, vol. 9, third ed., Wiley, New York, 1984, p. 881.
[4] J.B. Goodenough, Proc. IEE 104B (1957) 400.
[5] R. Lar, P. Ramakrishman, Trans. Ind. Ceram. Soc. 38 (1979) 166.
[6] D.J. Epstein, B. Frackiewucz, J. Appl. Phys. 29 (1958) 376.
[7] E. Koch, C. Wagner, Z. Phys. Chem. B34 (1936) 317.
[8] R.E. Carter, J. Am. Ceram. Soc. 44 (1961) 116.
[9] L.C.F. Blackman, J. Am. Ceram. Soc. 42 (1959) 143.
[10] P. Reijnen, in: G.H. Stewart (Ed.), Science in Ceamics, vol. 3, Academic Press, London, 1967, p. 245.
[11] M. Paulus, in: Y. Hoshino (Ed.), Proceedings of the International Conference on Ferrites, Kyoto, 1970, University of Toyko Press, 1971, p. 114.
[12] G.A. El-Shobaky, A. Ibrahim, Thermochim. Acta 132 (1988) 117.
[13] G.A. El-Shobaky, G.A. Fagal, A. Abd El-Aal, A.M. Ghozza, Thermochim. Acta 256 (1995) 429.
[14] G.A. El-Shobaky, F.H.A. Abdalla, A.F. Zikry, Thermochim. Acta 289 (1996) 81.
[15] G.A. El-Shobaky, F.H.A. Abdalla, A.M. Ghozza, Thermochim. Acta 292 (1997) 123.
[16] G. Turky, M.S. Selim, G.A. El-Shobaky, Solid State Ionics 140 (2001) 73.
[17] H.G. El-Shobaky, Thermochim. Acta 343 (2000) 145.
[18] G.A. El-Shobaky, N.R.E. Radwan, F.M. Radwan, Thermochim. Acta 380 (2001) 27.
[19] H.G. El-Shobaky, N.R.E. Radwan, Thermochim. Acta 398 (2003) 223–231.
[20] B.D. Cullity, Elements of X-Ray Diffraction, Addison-Wesley Publishing Co. Inc., 1967 (Chapter 14).
[21] W. Jander, Z. Allgem. Anorg. Chem. 163 (1927) 1.
[22] A.M. Ginstling, B.I. Brounstein, J. Appl. Chem. 23 (1950) 1327.
[23] T. Ozawa, J. Thermal Anal. 2 (1970) 301.
[24] B.C. Harding, Phil. Mag. 16 (1967) 1039.
[25] R.E. Carter, F.D. Richardson, J. Met. 6 (1954) 1244.
[26] Y.P. Gupta, L.J. Wevrick, J. Phys. Chem. Solids 28 (1967) 811.